ADAS-EU

ADAS for fusion in Europe

Grant: 224607

Hugh Summers, Martin O'Mullane, Francisco Guzman and Luis Menchero

Scientific progress report 4

April 13, 2012

Workpackages : 3-3, 4-1, 8-4, 9-1, 9-2, 9-3, 11-1, 26-1-4,S1, S4
Category : DRAFT

Scientific progress report 4

Hugh Summers, Martin O'Mullane, Francisco Guzman and Luis Menchero

Department of Physics, University of Strathclyde, Glasgow, UK

Abstract: *The report reviews scientific task completion for project months 19-24*

Contents

1 Overview **3**

2 Individual contributions **4**

2.1 Hugh Summers: Dielectronic recombination for special features and BBGP 4

2.1.1 Doubly excited states and adf04 datsets 4

2.1.2 Preparing BBGP drivers 5

2.2 Martin O'Mullane: Code developments and ITER engagements 5

2.3 Francisco Guzmán: Molecular CR modelling 5

2.3.1 Ion impact excitation data 6

2.3.2 Ar MGI time dependent model 6

2.3.3 Completion of report science_4 6

2.4 Luis Menchero: Atomic structure of beam atoms in fields 6

2.4.1 Data of ion-impact excitation adf02 6

2.4.2 Preparation of a programming code to calculate differential cross-sections 7

2.5 Nigel Badnell: Electron impact collision cross sections 7

A ADAS Theme 5 supplementary material for the report **8**

B Excitation cross sections from classical and semiclassical methods in a wide energy range for the reactions
(Li^{3+},Ne^{10+},Ar^{18+}) + H($1s$) →(Li^{3+},Ne^{10+},Ar^{18+}) + H(n) **14**

Preface

This scientific report is one of a series of six such reports, deliverable under the ADAS-EU project, which summarise the scientific achievements of the project over the preceding six months.

H P Summers
21 June 2010

Chapter 1

Overview

Chapter 2

Individual contributions

2.1 Hugh Summers: Dielectronic recombination for special features and BBGP

A main theme of ADAS-EU is the analysis of special spectroscopic features. The conceptual design of a code package comprising an ADAS feature generator (AFG) along with a framework for feature synthesis (FFS) was prepared by Whiteford and Meigs, and followed through in the PhD programme of Nicholas, supported by Summers. The design was fully realised and put into application in a series of spectroscopic studies drawn from astrophysics and fusion. The full description is available as ADAS-EU report PUBL1. The system uses ADAS theoretical emissivity features as the basis for the special feature model input. One of the most widely exploited special features in fusion (and astrophysics) is the resonance and associated lines of the helium-like system together with the satellite lines to them in the lithium-like system. The main activity in this time period was the refinement of the ADAS codes for preparing the special feature datasets of the above form, described in section 2.1.1. Additional work was carried out on the infrastructure codes for the Burgess-Bethe-general program (BBGP) approximation to state selective dielectronic recombination, described in section 2.1.2.

2.1.1 Doubly excited states and adf04 datsets

The He-like/Li-like satellite line special feature is a special case of a more general construct, namely, spectral lines associated with transitions of a parent ion core with a spectator electron in a higher excited Rydberg state (the $z-1$ times ionised system) and the lines associated with the transitions of a parent ion core in isolation (the z times ionised system). The former doubly excited states may be formed by dielectronic recombination of the z times ionised system or by (inner) shell excitation of the $z-1$ times ionised system. Three ADAS code package developments, which have been in existence for some years, are assigned to this activity, namely: ADAS703 (which prepares *adf04* datsets from AUTOSTRUCTURE calculations inclduing Auger and resonance capture rates for autoionising states); ADAS705 (which matches, assembles and bundles *adf04* datasets from various sources); ADAS706 (which executes population calculations from *adf04* inputs and prepares the *pec* and *fpec* outputs in ADAS formats *adf15* and *adf40*. The activity in this period was firstly the rationalising of the subroutines of these packages to match latest AUTOSTRUCTURE versions, updated ADAS code infrastructure, and to refine the models suitably for the Nicholas special feature handler described in the introduction of section 2.1. The amalgamation of divergent variants of core subroutines and the centralising in top-level ADAS general libraries was done in Jul. and Aug. The revised ADAS703 code was fully operational, as an offline version, by Dec., of which the subroutines *xxdata_olg.for* and *g5astj.for* were the large developments. Energy level and collisional rate coefficient matching and merging between different *adf04* datasets is a key requirement for atomic physics population modelling since best data usually comes from laborious patching of good, partial data from multiple sources. The present case is typical, where the best available Auger data comes from AUTOSTRUCTURE, but the best electron impact excitation data from R-matrix calculations. The ADAS705 codes aid this process and were updated and revised in this period. The major revision of the population code ADAS706 took place in Nov. and Dec. This code is significantly different from the familiar population codes in ADAS, since it

must maintain consistency in handling radiated power from the intermediate-state-resolved and unresolved aspects of dielectronic recombination as one progresses to higher n-shells. The codes were in a working state by the end Dec. 2010, sufficient for Nicholas to go to completion on his thesis and the satellite line special feature provision within AFG/FFS and ADAS-EU workpackage and ADAS capabilities descibed in detail in PUBL1. Futher development work on the codes is anticipated and their positioning in off-line/on-line ADAS in later work periods.

2.1.2 Preparing BBGP drivers

Collisional-radiative (CR) and generalised-collisonal-radiative (GCR) modelling of atomic population structure requires extensive state-selective dielectronic recombination data. ADAS uses a number of approximations which stem from the original code which Burgess [**?**] used for his zero-density general formula. For the highest precision, possible for moderately complex systems up to ∼ Al-like, *adf09* tabulations produced by AUTOSTRUCTURE are used. For more complex systems, ADAS defaults to a variant of the Burgess code developed by Summers [**?**]. More recent studies [**?**, **?**] indicate the effectiveness of the approach, especially if it is tuned to specific systems and includes non-dipole as well as dipole parent transitions. This is called the Burgess-Bethe-general program (BBGP) approximation. ADAS has a strategy for use of BBGP for the lifting of the ADAS baseline database for medium/heavy systems where the *adf09* tabulations and calculation become excessive. An ADAS data format *adf42* has been specified to drive BBGP calculations. In this period, the specification of *adf42* wqas refined and the key access routine *xxdata_42.for* prepared. Further development will be done on bringing BBGP into play in later periods.

2.2 Martin O'Mullane: Code developments and ITER engagements

2.3 Francisco Guzmán: Molecular CR modelling

A new ADAS molecular format structure based in ADAS atomic files *adf* plus a number indicative of the class of data they contain. The new files are called *mdf* from *molecular data files* plus a number and they contain the specific formats that include the peculiarities of molecules descriptions. This is described in the document **PUBL6**, which will be a detailed technical and scientific document where **Theme 5** achievements will be described and which is part written (contents in Appendix A).

A compilation of molecular data from electron and ion-impact data provided by Professor R. Janev[**?**] together with new improvements has been implemented in the new formats and reading routines are available. These data that are now cross sections in a "raw" form and will be processed over the next semester to obtain the corresponding Maxwell rate coefficients with the corresponding interpolation and extrapolation to the required energy ranges. These data will be in the molecular format files *mdf02*. They are structured to contain all the information of a molecular system (which means all the molecular species derived from a "initial" molecule) and are arranged first with the derived species information, followed with the process information, then is electronic states information and finally the data for each transition comes preceded by some parameters which give information of each transition. The data here can be vibrationally resolved or unresolved and cross section or maxwellian coefficients provided their correct identification by the reading routines. **These actions correspond to the partial completion of milestone SCI51 concerning the transfer to ADAS H_2 data base and vibronic population model , which was not completed at the previous stage is partially done now regarding to the data base transfer. That correspond to the completion of work package task 17-1 concerning to the definitions of the new ADAS formats**.

Reading routine *xxdatm_02* has been created as well and will pass the information to the programs which will organize it in the maxwellian coefficients that will be presented in a vibrationally resolved or unresolved way. Interpolation and extrapolation routines *intrp* and extrap have also been created. Extrapolation is using physical accepted laws: over-barrier model for CX[**?**], Bethe approximation for ionization[**?**] and prof. R. K. Janev[**?**] fitting formulas together with splines for excitation cross sections.

Subroutine *thermrat* is performing the Maxwell integrations of cross section. This make use of the previously cited routines. The ion-impact rate coefficients should be in a double temperature function that have been already defined. The interpolation and integration routines have been already programmed and the final implementation in the

routine ADAS902 of new ADAS900 series will be done during the next period. **This makes the basis of the future collisional-radiative model (milestone SCI52) that will be completed at the beginning of 2012.**

2.3.1 Ion impact excitation data

The data from the subcontracts depend on calculations that carry out an undetermined amount of time. Part of the data from subcontract S5 corresponding to excitation cross sections for Li^{3+}, Ar^{18+} and Ne^{10+} collisions with Hydrogen have been successfully transfer and embedded in the database as was included in the previous report. These data have been obtained from the joining of the different method in a final recommended data set. ADAS-EU report concerning this tack is attached in appendix B. **That correspond to the milestone SCI25 which concerns to the embedding of the of the charge exchange cross section data from subcontracts S5 and the re-optimizing of the universal parametric forms and partially completion of work package task 9-1**.

Charge exchange data for Kr^{36+} will be given over next six month period (February-March 2011). Dr. Francisco Guzmán (under the supervision of ADAS staff) have been in communication with the subcontract beneficiaries due to his background in charge exchange calculations. New calculations of AOCC data will be provided as well for Ne and Ar during next year. Universal parametric form will be re-optimized once the data are available.

2.3.2 Ar MGI time dependent model

A collaboration with FZJ staff Dr A. Huber and M. Lehnen has been started on Massive Gas Injection (MGI) studies.

The necessity to quantify the radiated power during MGI can be covered with the use of the time dependent ADAS transient ionization program ADAS406. This program calculates the time dependent radiated power for an initial neutral population of impurities in an homogeneous plasma.

A simple model using Ar injection in JET has been made by Dr. F. Guzmán which makes use of ADAS406. Departing from a radial profile of temperature and density coming from a real plasma, Ar abundances are calculated at each time step in each point of a grid in radius. These abundances are convoluted with the neutral Ar attenuation as it penetrates the plasma and new abundances are obtained in an iterative procedure. Radiated power is calculated at each time step from these final abundances.

These model has been in developing stage during this period . An IDL code have been created which allows to obtain the abundances given an input temperature and density radial profile. Next stage, regarding convolution with attenuation model is in progress.

As a future work, new improvement in the model are foreseen consisting in account for the increase of the local density from the ionization of Ar.

This is included in the on-site work responsibilities of F. Guzman as PDRA to assist in modelling and analysis at their placement sites.

2.3.3 Completion of report science_4

The work package task 26-1-4 comprises the completion of this report.

2.4 Luis Menchero: Atomic structure of beam atoms in fields

2.4.1 Data of ion-impact excitation adf02

Data for ion-impact excitation cross sections of collisions of fully striped ions of hydrogen, helium, lithium, berilium and higher charged against atomic hydrogen were stored in an *adf02* file. The cross sections were taken from the

theoretical and experimental data collected in reference [**?**] and interpolated and extrapolated using the proposed fitting formula in the report. Cross sections are resolved to any individual n main quantum number.

2.4.2 Preparation of a programming code to calculate differential cross-sections

A prototype code was programmed to calculate the differential cross sections $\frac{d\sigma}{d\theta}$ as a function of the deflection angle of the projectile θ: *difampl*. The program splits in two steps.

The first part, *deflection*, calculates the deflection function: the outgoing angle *theta* as a function of the classical impact parameter. For that task it uses the semiclassical scattering formula for the motion of the nuclei, which consists in the integration of a function of the interacting potential between both nuclei, which is approximated as central. The program allows the deflection function to be multivaluated if the potential has different behavior (attractive or repulsive) in different regions of the space, such multivaluation will lead to interference terms in the calculation of the differential amplitudes.

In the second part of the program, *difampl*, the differential amplitudes versus the scattering angle are obtained using the deflection function calculated in the previous step. If the deflection function is multivaluated an interference should be calculated, adding the transition amplitudes for the different classical impact parameters which lead to the same deflection angle, so for a proper work they should be stored and used the transition amplitudes and no the probabilities.

The ground of this program will be used for atoms in plasmas, when they are collisioning non isotropically, for example in the beam injectors, where there is a big directionality of the collisions. *difampl* is a necessary tool to build the collision radiative model of the atoms in the beam.

2.5 Nigel Badnell: Electron impact collision cross sections

Activities of Badnell relate to the Electron Collision Working Party (ECWP) and are to be found in the document ECWP1.

Bibliography

[1] A. Burgess. 'A General Formula for the Estimation of Dielectronic Recombination Co-Efficients in Low-Density Plasmas'. Astrophys. J., **141**(5) (1965) 1588–1590. doi:10.1086/148253

[2] H. P. Summers, K. Behringer and L. Wood. 'Recombination of Neon-Like and Adjacent Ions in Plasmas'. Phys. Scr., **35**(3) (1987) 303–308. doi:10.1088/0031-8949/35/3/013

[3] N. R. Badnell, M. G. O'Mullane, H. P. Summers, Z. Altun, M. A. Bautista, J. Colgan, T. W. Gorczyca, D. M. Mitnik, M. S. Pindzola and O. Zatsarinny. 'Dielectronic recombination data for dynamic finite-density plasmas I. Goals and methodology'. Astron. Astrophys., **406**(3) (2003) 1151–1165. doi:10.1051/0004-6361:20030816

[4] H. P. Summers, W. J. Dickson, M. G. O'Mullane, N. R. Badnell, A. D. Whiteford, D. H. Brooks, J. Lang, S. D. Loch and D. C. Griffin. 'Ionization state, excited populations and emission of impurities in dynamic finite density plasmas: I. The generalized collisional-radiative model for light elements'. Plasma Phys. Control. Fusion, **48**(2) (2006) 263–293. doi:10.1088/0741-3335/48/2/007

[5] R. K. Janev, D. Reiter and U. Samm. 'Collision and Radiative Processes in Hydrogen Plasmas (in progress)' (2011). Private communication

[6] B. H. Bransden and M. C. H. McDowell. *Charge Exchange and the theory of Ion-Atom Collisions*. OXford, Clarendon (1992). ISBN 9780198520207

[7] H. Bethe. 'Zur Theorie des Durchgangs schneller Korpuskularstrahlen durch Materie'. Annalen der Physik, **397** (1930) 325–400. doi:10.1002/andp.19303970303

[8] R. Janev and J. Smith. 'Cross sections for collision processes of hydrogen atoms with electrons, protons and multiply charged ions. Atomic and Plasma-Material Interaction Data for Fusion . Volume 4.' Technical report, IAEA, Vienna (1993)

Appendix A

ADAS Theme 5 supplementary material for the report

[1] ADAS-EU/REPORTS_PUBL/PUBL_6/ pages 1-6

-

ADAS-EU R(12)PU06

ADAS-EU
ADAS for fusion in Europe

Grant: 224607

F. Guzmán

PUBL6: The ADAS molecular population model for fusion plasmas

1 Feb 2012

Workpackages : 26-6-6
Category : DRAFT – CONFIDENTIAL

PUBL6: The ADAS molecular population model for fusion plasmas

F. Guzmán

Department of Physics, University of Strathclyde, Glasgow, UK

Abstract: *Public report for ADAS_EU*

Contents

1 Introduction **4**

1.1 Molecules in plasmas . . . 4

1.2 H_2 System . . . 4

1.3 Isotopic Scaling . . . 4

2 H_2 data **5**

2.1 Type of data and quality . . . 5

2.2 Fitting formulas . . . 5

2.3 Scaling and classical models . . . 5

2.3.1 Scaling . . . 5

2.3.2 Classical Models . . . 5

2.4 Maxwell rates . . . 5

2.4.1 Single maxwellian integrations for electron-impact collisions . . . 5

2.4.2 Double maxwellian integrations for ion-impact collisions . . . 5

3 Collisional-Radiative model for molecules **6**

3.1 Molecular Generalized Collisional-Radiative Model . . . 6

3.1.1 Time Scales . . . 6

3.1.2 Collisional Radiative model . . . 11

3.1.3 Vibrational resolution in molecular GCR . . . 12

3.2 Source terms . . . 12

3.3 Other Molecular Collisional-Radiative Models . . . 12

4 ADAS9xx: The molecular ADAS **13**

4.1 Structure and Diagrams . . . 13

4.1.1 MDF: The Molecular ADAS format . . . 13

4.1.2 Index of parameters in *mdf* files . . . 17

4.2 The Molecular ADAS routines . . . 17
4.2.1 Scaling, widening and resolving . . . 17
4.2.2 The collisional-radiative routines . . . 17

5 Results **18**
5.1 Checking in the experimental plasma . . . 18
5.2 The molecular challenge. ADAS9xx: a general molecular software . . . 18

A MDF data formats **20**
A.1 *mdf00*: general parameter information files and potentials curves . . . 20
A.1.1 potentials . . . 20
A.1.2 vibrational energies . . . 20
A.1.3 Franck-Condon Factors . . . 24

B IDL procedures **26**

C FORTRAN subroutines **27**
C.1 ADAS902 . . . 27
C.1.1 adas902.for . . . 28
C.1.2 thermrat.for . . . 46
C.1.3 intrp.for . . . 53
C.1.4 extrap.for . . . 57
C.1.5 dstform.for . . . 61
C.1.6 wrt_mdf04.for . . . 63
C.1.7 fcf.for . . . 67
C.1.8 rd_enu.for . . . 69

D Shell scripts **71**

E Fitting Formulas **72**

Appendix B

Excitation cross sections from classical and semiclassical methods in a wide energy range for the reactions

$(Li^{3+},Ne^{10+},Ar^{18+}) + H(1s)$ $\rightarrow(Li^{3+},Ne^{10+},Ar^{18+}) + H(n)$

Excitation cross sections from classical and semiclassical methods in a wide energy range for the reactions
$(Li^{3+},Ne^{10+},Ar^{18+}) + H(1s)$
$\rightarrow(Li^{3+},Ne^{10+},Ar^{18+}) + H(n)$

F. Guzmán

June 18, 2010

Abstract

Here is detailed how the excitation cross section recommended data that are stored in the *adf01* files *qex#h0_uam#li3.dat*, *qex#h0_uam_n2n3#li3.dat*, *qex#h0_uam#ne10.dat* and *qex#h0_uam#ar18.dat* corresponding to the collisions of fully stripped Li, Ne and Ar with ground state H have been obtained from the different semiclassical and semiclassical calculation [1, 2]. Joining and interpolation from the different energy ranges of each method is detailed. A brief overview of the methods is also included.

1 Introduction

Excitation cross sections are presented for reactions:

$$Li^{3+} + H(1s) \rightarrow Li^{3+} + H(n) \quad (1)$$
$$Ne^{10+} + H(1s) \rightarrow Ne^{10+} + H(n) \quad (2)$$
$$Ar^{18+} + H(1s) \rightarrow Ar^{18+} + H(n) \quad (3)$$

These data have been previously calculated in [3, 1, 2]. They come from OEDM, CTMC (Microcanonical and Hydrogenic distributions) and monocentric-Bessel calculations. All these have been combined and interpolated to obtain one unique data set in a recommended energy range for each reaction. The interpolation have been done using Akima splines that behaves better than cubic splines (for a study of differences see for example [4]). The energy range differs in the reactions as calculations have different validity for the different ions and the molecular basis should have more functions to describe excitation as the nuclear charge of target increases what makes difficult to describe excited states with OEDM methods. A brief overview of the methods used will be presented in next section. After, energy range and considerations for each of the reactions above are stated.

2 Overview of theoretical methods

Here a basic overview of the method used for calculations is given. These have been OEDM, CTMC (with microcanonical and hydrogenic distributions) and Monocentric-Bessel method. Knowledge of the internal mechanism of this calculations is essential to correctly join the data in their different application energy range.

Monocentric-STO formalism calculation also exist for Li [5] and Ar [1] but the data are much fewer and give the same results than Bessel in their validity range for Li and and Ar and have problems from insufficient basis description at low impact velocities in Ar. Because it, Monocentric-STO calculations have not been chosen to be in the *adf01* files. They provide a good checking of Monocentric-Bessel calculation though.

2.1 Semiclassical methods

2.1.1 One Electron Diatomic Molecule molecular orbitals

The molecular orbitals OEDM are eigenfunctions of the Born-Oppenheimer Hamiltonian:

$$H_{el}\Phi_j(\boldsymbol{r},R)=\left(-\frac{1}{2}\nabla^2-\frac{Z_A}{r_A}-\frac{Z_B}{r_B}+\frac{Z_BZ_A}{R}\right)\Phi_j(\boldsymbol{r},R)=E_j^{cc}(R)\Phi_j(\boldsymbol{r},R) \tag{4}$$

Due to the cylindrical symmetry of the system this eigenfuctions can be described in elliptic confocal coordinates(λ,μ,ϕ)[6]. The wave function can be separated in these coordinates for the wavefunctions $\Phi_j^{OEDM}(\boldsymbol{r},R)=\Lambda_j(\lambda)M_j(\mu)\Omega_j(\phi)$ and the solution of (4) is:

$$\begin{aligned}
\Lambda_j(\lambda,R) &= \left(\lambda^2-1\right)^{m/2}(\lambda+1)^{\sigma_j}\,\mathrm{e}^{-p'_j\lambda}\sum_{t_j=0}^{\infty}g_{t_j}(R)\left(\frac{\lambda-1}{\lambda+1}\right)^{t_j}\\
&\quad \text{with } \sigma_j=R\frac{Z_A+Z_B}{2p'_j}-m-1\\
M_j(\mu,R) &= \sum_{s_j=0}^{\infty}f_{s_j}(R)P^m_{m+s_j}(\mu)\\
\Omega_j(\phi) &= \begin{cases}(4\pi)^{-1/2}\left(\mathrm{e}^{im\phi}\pm\mathrm{e}^{-im\phi}\right) & m\neq 0\\ (2\pi)^{-1/2} & m=0\end{cases}
\end{aligned} \tag{5}$$

where P_l^m are the Legendre Polynomials (not normalized) and f_{s_j}, g_{t_j} are the expansion coefficients. OEDM orbital are bicentric.

As OEDM only describe bound orbitals, ionization cannot be described by these basis. When ionization cross sections are comparable to charge exchange has been shown that the group of highest OEDM takes the ionization flux as a charge exchange and start to give electron loss as result [7]. This restrict this method to energies where ionization is negligible compared to capture.

2.1.2 Monocentric-Bessel orbitals

In this formalism the coordinate space is restricted to an sphere of radius r_{max} where the radial components of the wavefunction are $R_{\epsilon_n lm}(r\geq r_{max})=0$. In this way the continuum spectra remains discretized and

these wavefunction will describe the ionization and electron loss. One can employ a spherical Bessel functions basis $\{j_l\}$ to describe the wavefunctions [8] and the eigenfunctions from 4 are:

$$\Phi(\boldsymbol{r}) = j_l(kr)Y_l^m(\theta,\phi) \tag{6}$$

where $Y_l^m(\theta,\phi)$ are the spherical harmonics. The Bessel functions have the correct asymptotic behavior for the stationary continuum modes.

At low velocities, where the ionization is no longer important the ionization pseudostates get capture flux so they reproduce electron loss. At this velocities the high excitation channels ($n \geq 4$) get populated by capture flux, although not so strongly as other monocentric treatments as Slater Type Orbitals get. This gives a low energy limit in the range of application of this formalism.

2.1.3 Eikonal formalism

At big enough impact energies nuclei motion can be approach by straight trajectories:

$$\boldsymbol{R}(t) = \boldsymbol{b} + \boldsymbol{v}\,t$$

with $\boldsymbol{b}$ the impact parameter vector and t the classical time $t = Z/v$ (Z is the axial coordinate were the collision takes place). Electronic motion is described by the wavefunctions $\Psi(\boldsymbol{r};t)$ that are solution of the eikonal equation:

$$ß\left(\left.\frac{\partial\Psi(\boldsymbol{r};t)}{\partial t}\right|_r\right) = H_{el}\Psi(\boldsymbol{r};t) \tag{7}$$

Here, $\Psi(\boldsymbol{r};t)$ is expanded in molecular orbitals (exact, variational):

$$\Psi(\boldsymbol{r},t) = \mathrm{e}^{iU(\boldsymbol{r},R)}\sum_j^N a_j(t)\Phi_j(\boldsymbol{r};R)\exp\left[-i\int^t E_j(t')dt'\right] \tag{8}$$

where U is the Common Translation factor (CTF)[9] in the case of OEDM and $U = 0$ in case of Bessel treatment.

Solving, a coupled equation system is obtained:

$$\begin{aligned}\frac{\mathrm{d}a_k(t)}{\mathrm{d}t} &= \sum_j a_j(t)\Bigg(\left\langle\Phi_k\left|H_{el} - \mathrm{i}\frac{\partial}{\partial t}\right|\Phi_j\right\rangle + \left\langle\Phi_k\left|\frac{1}{2}(\nabla U)^2 + \frac{\partial U}{\partial t}\right|\Phi_j\right\rangle + \quad (9)\\ &- \mathrm{i}\left\langle\Phi_k\left|-\frac{1}{2}\nabla^2 U - \nabla U\cdot\nabla\right|\Phi_j\right\rangle\Bigg)\exp\left[-i\int_0^t (E_j(t') - E_k(t'))dt'\right] \quad (10)\end{aligned}$$

Here, the first term on the right are the dynamical coupling between states and the second and third term are the CTF correction to energy and couplings respectively. Those correction do not apply in the case of monocentric formalism. This multiplied by a phase that depends on the energy difference between the orbital and optimize the transitions in the avoided coupling by the Massey criteria.

The cross section are obtained from the probabilities:

$$\sigma_{nlm}^{A,B}(v) = 2\pi\int |a_{nlm}^{A,B}(v,b,t\to\infty)|^2 b\mathrm{d}b. \tag{11}$$

2.2 The Classical method CTMC

This method was developed for first time in [10] and improved in [11]. Here the electronic motion is described by a statistical distribution of N punctual charges that do not interact:

$$\rho(\boldsymbol{r},\boldsymbol{p},t)=\frac{1}{N}\sum_{j=1}^{N}\delta\left(\boldsymbol{r}-\boldsymbol{r}_j(t)\right)\delta\left(\boldsymbol{p}-\boldsymbol{p}_j(t)\right) \tag{12}$$

The system coordinate fulfill the Hamilton Equations:

$$\left.\begin{array}{rl}\dot{r}_j(t)= & \frac{\partial H}{\partial p_j(t)}\\ \dot{p}_j(t)=- & \frac{\partial H}{\partial r_j(t)}\end{array}\right\} \tag{13}$$

An the probability is the distribution of trajectories at the end of the collision:

$$P_{c,e,i}(v,b)=\int d\boldsymbol{r}\int d\boldsymbol{p}\,\rho_{c,e,i}(\boldsymbol{r},\boldsymbol{p},t_{max})=\frac{N_{c,e,i}}{N_{\text{Total}}} \tag{14}$$

The cross section is then:

$$\sigma_{c,e,i}(v)=2\pi\int_0^\infty db\,b\,P_{c,e,i}(v,b) \tag{15}$$

where c,e,i stand for capture, excitation or ionization. As this is a classical formalism, initial conditions should be given. These should be the most similar possible to the quantal distribution in momentum and coordinate spaces. Several solution have been proposed to this problem, most important of them (and here used) are the microcanonical and Hydrogenic (or Hardie-Olson) distributions:

- Microcanonical Distribution that describes exactly the momentum space but has a classically forbidden area to $r>r_{max}$ where $r_{max}=-Z/E_0$:

$$\rho^m(\boldsymbol{r},\boldsymbol{p};E_0)=\frac{(2\left|E_0\right|)^{5/2}}{8\pi^3 Z_H^3}\delta\left(\frac{p^2}{2}-\frac{Z_H}{r}-E_0\right) \tag{16}$$

- Hydrogenic Distribution this is a combination of microcanonical distribution at different energies that fit the quantal distribution and with the condition that $\langle E\rangle=E_0$:

$$\rho(\boldsymbol{r},\boldsymbol{p})=\sum_{j=1}^{N_j}w_j\rho^m(\boldsymbol{r},\boldsymbol{p};E_j) \tag{17}$$

  Another continuous distributions have been proposed but will not be treated here (Gaussian, Rackovic, Cohen, Eichenauer).

Classical method start to be adequate when the kinetic energy of the collision can be compared with the kinetic energy of the electron. That is around $E\sim 25keV/amu$. Microcanonical distribution describes better the low levels where the momenta distribution description is more important. At higher levels a good description of the quantal tail in the classically forbidden part of the spatial microcanonical distribution is needed as a big part of the excitation and the ionization come from these trajectories. For this is needed the combination of several microcanonical distributions. A good description of partial cross sections is achieved by a good combination of microcanonical and hydrogenic distribution for the different n levels.

3 Recommended data

3.1 $Li^{3+} + H(1s) \rightarrow Li^{3+} + H(n)$

The original data are presented in figure 1 where in the X axes is represented the collision velocity in atomic units (a.u.). Here OEDM method is runs only until $v = 2$a.u. ($E \sim 100$keV/amu) but it get contaminated by ionization from 1a.u.(~ 25keV/amu) approximately. Bessel get adequate from ~ 100keV/amu [2, 1], so an interpolation seems adequate between those values. For higher n, OEDM calculation has not a big enough basis to reproduce these levels so CTMC has to be applied. The classical treatment cannot go much further down without purely quantal effects taking place. So a low limit of 16keV/amu has been imposed according to interpolation.

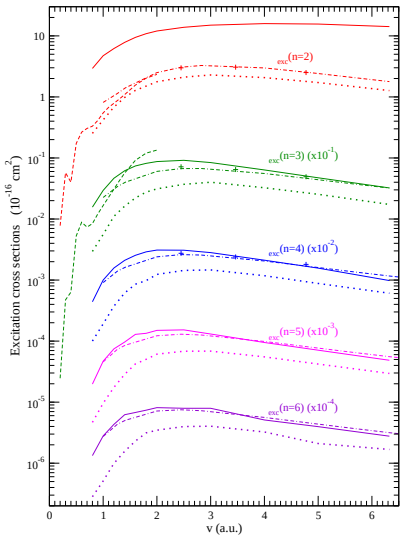

Figure 1: Partial cross section for the reaction 1 in function of internuclear relative velocity v. OEDM:(—) P175; CTMC: microcanonical $(\cdots)$, hydrogenic $(- - -)$: monocentric-Bessel $(- - \cdot)$[3];monocentric-STO$(+)$[5]. From [1]

Interpolation of data has been done joining Bessel and OEDM calculation in $n = 2, 3$ and Bessel and CTMC (hydrogenic) for $n \geq 4$. To that set an Akima Spline has been applied **to the complete range of energies** to probe that the result changes smoothly with energy. The points in the gap between the two methods have been filled with the points resulting from the spline.

Two files have been created:

qex#h0_uam#li3.dat that has an energy range 15.99 keV/amu$\leq E \leq$ 999.35 keV/amu. Interpolated recommended data from $n = 2$ to

$n = 6$ are given.

qex#h0_uam_n2n3#li3.dat that has an energy range 1.00 keV/amu$\leq E \leq$ 999.35 keV/amu. Interpolated recommended data from $n = 2$ to $n = 3$ are given. This have been done to take advantage of that OEDM method is valid for much lower energies than CTMC method.

The energy ranges in which each method is used and the interpolation values are given in the tables 1 and the interpolation range is the same for both files. The final recommended cross sections are presented in figure 2. In table 1 and tables 2 and 3 interpolation means that the interpolated points have been taken from the spline fit, that runs over the whole energy range considered.

Table 1: Energy ranges (keV/amu) in which each method is applied. CTMC(m) refers to microcanonical initial distribution and CTMC(h) refers to hydrogenic distribution. Interpolations are done by Akima splines. Interpolation means that the interpolated points have been taken from the spline fit, that runs over the whole energy range considered.

n	Method(E)	Method(E)	Interp. Energy
2	OEDM ($1 \leq E \lesssim 100$)	Bessel ($100 \lesssim E \lesssim 1000$)	
3	OEDM ($1 \leq E \lesssim 30$)	Bessel ($50 \lesssim E \lesssim 1000$)	$30 \lesssim E \lesssim 50$
4	CTMC(h) ($16 \lesssim E \lesssim 50$)	Bessel ($140 \lesssim E \lesssim 1000$)	$50 \lesssim E \lesssim 140$
5	CTMC(h) ($16 \lesssim E \lesssim 50$)	Bessel ($150 \lesssim E \lesssim 1000$)	$50 \lesssim E \lesssim 150$
6	CTMC(h) ($16 \lesssim E \lesssim 64$)	Bessel ($150 \lesssim E \lesssim 1000$)	$64 \lesssim E \lesssim 150$
total	OEDM ($1 \lesssim E \lesssim 64$)	Bessel ($150 \lesssim E \lesssim 1000$)	$64 \lesssim E \lesssim 150$

The ranges change with different n as to ensure smoothness of the cross section is needed to join in different ranges. Validity and smoothness have been checked in each n. Total cross sections do not have to correspond to the simple summation of the partial as total OEDM cross sections includes all the probability flux that goes to excitation and CTMC includes all the statistics (CTMC goes to levels as high as $n = 30$ in capture and excitation).

In the figure 2 are represented the final recommended cross section and the values used in the *adf01* files is signaled with symbols. It is possible to see that the value of the cross sections in Bessel calculation at low energy first decrease and the increases again as a result of the contamination from capture. The reason of the decreasing in firs place remains unknown but could be due to an effect of the incompleteness of the basis there.

3.2 $\mathbf{Ne}^{10+} + \mathbf{H}(1s) \rightarrow \mathbf{Ne}^{10+} + \mathbf{H}(n)$

The original data are presented in figure 3 and the same considerations as in the Li case are taken with respect to the ranges in which the differnt methods apply. As we need a huge basis here OEDM can only describe until n=2. The limitation of methods is as Li case and the interpolation with splines has been done in the same way. Here all the data comes from [1]. The energy ranges are given in table 2 and the final recommended data are presented in figure 4. The file created is *qex#h0_uam#ne10.dat*.

Here as no other data were available a summation had to be used for total cross section in the low energy range. However, this case is different

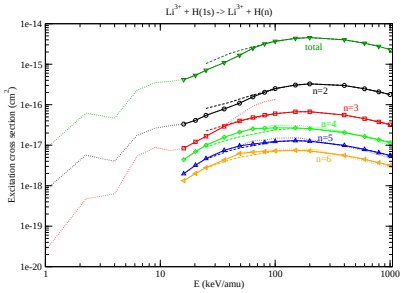

Figure 2: Partial final recommended cross section for the reaction 1 in function of collision energy. Low energy methods (CTMC,OEDM):(⋯); final recommended (solid line with symbols); monocentric-Bessel (−−).

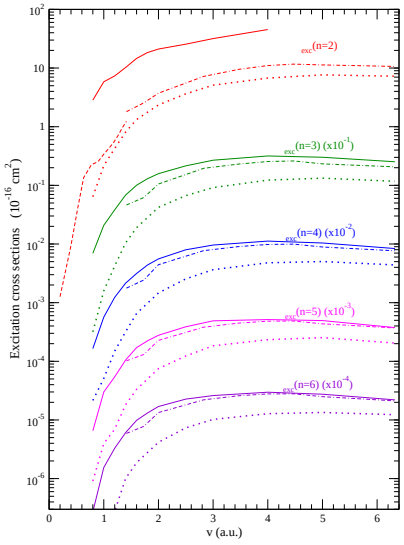

Figure 3: Partial cross section for the reaction 2 in function of internuclear relative velocity v. OEDM:(—) P310; CTMC: microcanonical (⋯), hydrogenic (− − −): monocentric-Bessel (− − ·). From [1].

that Li one as high excitation levels are many more levels of capture upper and one can approximate as that higher excitation levels for low energy will populated with negligible probability.

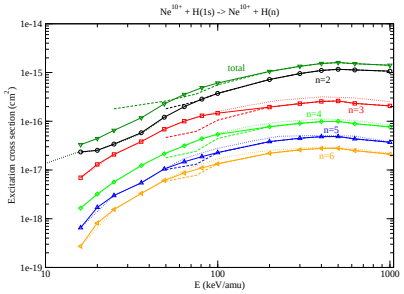

Figure 4: Partial final recommended cross section for the reaction 2 in function of collision energy. Low energy methods (CTMC,OEDM):$(\cdots)$; final recommended (solid line with symbols); monocentric-Bessel $(--)$.

3.3 $\mathbf{Ar^{18+} + H}(1s) \rightarrow \mathbf{Ar^{18+} + H}(n)$

The original data are presented in figure 5 as before. There are no OEDM calculation available here. The limitation of methods is as Li case and the interpolation with splines has been done in the same way. Here all the data comes from [1]. The energy ranges are given in table 3 and the final recommended data are presented in figure 6. The file created is *qex#h0_uam#ar18.dat*.

Here CTMC is really going from $E = 16$keV/amu but as there are some inconsistencies in $n = 2$ and $n = 3$ due to the fact that microcanonical distribution is chosen in $n = 2$ and hydrogenic in $n = 3$. Microcanonical data is adequate for $n = 2$ but not anymore for $n = 3$ calculations (see section 2.2), a hydrogenic one is used here but still this is not totally adequate here and gives to high cross sections at low energies crossing with the $n = 2$ curve as is seen in figure 6. This is clearly not correct and all data under 36 keV/amu have been eliminated to avoid inconsistencies. Again a summation is used for the total cross sections, the reason is the

Table 2: Energy ranges (keV/amu) in which each method is applied. CTMC(m) refers to microcanonical initial distribution and CTMC(h) refers to hydrogenic distribution. Interpolations are done by Akima splines. Interpolation means that the interpolated points have been taken from the spline fit, that runs over the whole energy range considered.

n	Method(E)	Method(E)	Interp. Energy
n=2	OEDM ($16 \leq E \lesssim 50$)	Bessel ($75 \lesssim E \lesssim 1$)	
n=3	CTMC(h) ($16 \leq E \lesssim 80$)	Bessel ($200 \lesssim E \lesssim 1$)	$80 \lesssim E \lesssim 200$
n=4	CTMC(h) ($16 \lesssim E \lesssim 80$)	Bessel ($200 \lesssim E \lesssim 1$)	$80 \lesssim E \lesssim 200$
n=5	CTMC(h) ($16 \lesssim E \lesssim 80$)	Bessel ($200 \lesssim E \lesssim 1$)	$80 \lesssim E \lesssim 200$
n=6	CTMC(h) ($16 \lesssim E \lesssim 80$)	Bessel ($200 \lesssim E \lesssim 1$)	$80 \lesssim E \lesssim 150$
total	Summation(n=2-n=6) ($16 \lesssim E \lesssim 50$)	Bessel ($75 \lesssim E \lesssim 1$)	

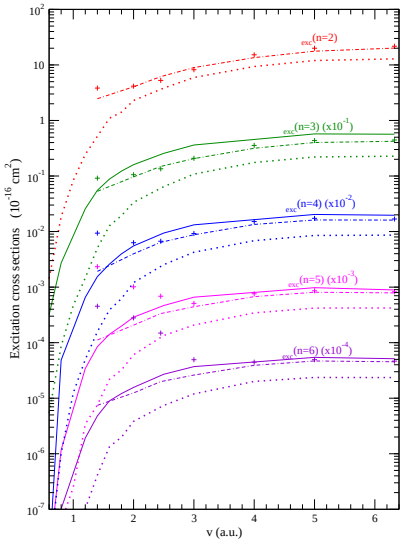

Figure 5: Partial cross section for the reaction 3 in function of internuclear relative velocity v. CTMC: microcanonical $(\cdots)$, hydrogenic $(---)$: monocentric-Bessel $(--\cdot)$;monocentric-STO$(+)$. From [1].

same than in the Ne case.

Table 3: Energy ranges (keV/amu) in which each method is applied. CTMC(m) refers to microcanonical initial distribution and CTMC(h) refers to hydrogenic distribution. Interpolations are done by Akima splines. Interpolation means that the interpolated points have been taken from the spline fit, that runs over the whole energy range considered.

n	Method(E)	Method(E)	Interp. Energy
n=2	CTMC(m) ($36 \leq E \lesssim 64$)	Bessel ($150 \lesssim E \lesssim 1$)	$64 \lesssim E \lesssim 150$
n=3	CTMC(h) (E $\lesssim$36)	Bessel ($150 \lesssim E \lesssim 1$)	$36 \lesssim E \lesssim 150$
n=4	CTMC(h) ($36 \lesssim E \lesssim 64$)	Bessel ($100 \lesssim E \lesssim 1$)	$64 \lesssim E \lesssim 100$
n=5	CTMC(h) ($36 \lesssim E \lesssim 80$)	Bessel ($150 \lesssim E \lesssim 1$)	$80 \lesssim E \lesssim 150$
n=6	CTMC(h) ($36 \lesssim E \lesssim 80$)	Bessel ($150 \lesssim E \lesssim 1$)	$80 \lesssim E \lesssim 150$
total	Summation(n=2-n=6) ($36 \lesssim E \lesssim 80$)	Bessel ($150 \lesssim E \lesssim 1$)	$80 \lesssim E \lesssim 150$

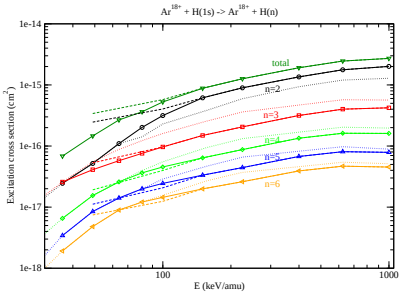

Figure 6: Partial final recommended cross section for the reaction 3 in function of collision energy. Low energy methods (CTMC):$(\cdots)$; final recommended (solid line with symbols); monocentric-Bessel $(--)$.

4 Final Remarks

In this paper is presented a summary of the actual method followed to join the data from different theoretical calculation to give a complete energy range set of cross sections. The different theoretical consideration to compensate the lack of a unique method to get fundamental cross sections *ab initio* have been exposed. Cross section in wide energies ranges are useful to get rates and apply collisional-radiative models. In spite of the lack of precision in the joining areas is expected that integration in thermal distribution and the correction of cascade effect will *smooth* this deficiencies.

References

[1] J. Suárez. PhD thesis, Universidad Autónoma de Madrid, 2005.

[2] L. F. Errea, L. Méndez, B. Pons, A. Riera, I. Sevila, and J. Suárez. *Phys. Rev. A*, 74:012722, 2006.

[3] I. Sevila. PhD thesis, Universidad Autónoma de Madrid, 2003.

[4] J. Fried and S. Zietz. *Phys. Med. Biol.*, 18:550, 1973.

[5] F. Martín. *J. Phys. B: At. Mol. Opt. Phys.*, 32:501–511, 1999.

[6] M. Abramowitz and I. A. Stegun. *Handbook of mathematical functions*. New York, Dover, 1965.

[7] L. F. Errea, C. Harel, C. Illescas, H. Jouin, L. Méndez, B. Pons, and A. Riera. *J. Phys. B: At. Mol. Opt. Phys.*, 31:3199, 1998.

[8] B. Pons. *Phys. Rev. A*, 63:01274, 2001.

[9] S. B. Schneiderman and A. Russek. *Phys. Rev.*, 181:311, 1969.

[10] R. Abrines and I. C. Percival. *Proc. Phys. Soc.*, 88:861, 1966.

[11] D. J. W. Hardie and R. E. Olson. *J. Phys. B: At. Mol. Phys.*, 16:1983, 1983.

-